12th Brazilian Congress of Manufacturing Engineering
May 10th-12th, 2023, Brasilia, DF, Brazil

EFFECTS OF PTA DEPOSITION PARAMETERS ON GEOMETRY AND HARDNESS OF AISI 316L SINGLE-TRACKS

Gustavo Scheid Prass[1, 2]
Pedro Weiss Mattioli[1]
Ana Sofia C. M. d'Oliveira[1]
[1]Federal University of Paraná, Department of Mechanical Engineering, Av. Cel. Francisco H. dos Santos, 100 - Jardim das Américas, Curitiba, PR, Brazil
[2]SENAI Innovation Institute in Manufacturing Systems and Laser Processing, R. Arno Waldemar Döhler, 308 - Santo Antônio, Joinville, SC, Brazil
e-mails: gustavo.prass@ufpr.br; pedrowmattioli@ufpr.br; sofmat@ufpr.br

Abstract. *Directed Energy Deposition (DED) is an Additive Manufacturing (AM) technology involving the layer-by-layer building of components close to their final geometry. One of the main applications of DED is the repair of metallic components, since the technique offers good control over composition and microstructure, minimizing the impact on the existing part. Typically, DED processes use an electric arc or high-density energy beam as a heat source and metallic powder or wire as feedstock. However, the control of geometrical features is more demanding than in machining processes, a consequence of the nature of the feedstock, the heat source and the process itself. Therefore, it is required to obtain continuous, defect-free single-track walls to manufacture multilayer walls and more complex geometries. In repair operations, the impact of the deposition process on the damaged component should be minimized. Within this context, Plasma Transferred Arc (PTA) is a well-known process for applying coating on metallic materials, guaranteeing a good metallurgical bond between the substrate and the deposited material. PTA-DED process has a low carbon footprint when compared with other processes and offers significant competitive advantages for which a known behavior of processing variables is required. This study is part of an ongoing project and it addresses the effects of deposition current and deposition velocity on the geometry of single-track AISI 316L. The relationship between processing parameters, processability, and hardness is identified and discussed as a useful database to select AM maintenance procedures. A Design of Experiment (DoE), for single-track AISI 316L, deposited on AISI 304L plates, varying two factors were adopted, deposition current (4 levels) and deposition velocity (3 levels), totaling 12 sets of parameters. Statistical analysis showed that both factors alter the dilution with the substrate, while a higher current increased the dilution the velocity had the opposite effect. The results also revealed that both deposition parameters greatly affected the wettability, hence the geometry of the single tracks. The DoE allowed for a good predictive estimate of the interaction with a part being repaired and the refurbishing of its geometry by AM. This research points out that the geometry, microstructure, and hardness of the first deposited track play an important role in the quality and properties of subsequent multilayer builds, required to recover the part geometry or even add functionalities.*

Keywords: *Additive Manufacturing; Directed Energy Deposition; Plasma Transferred Arc; Design of Experiments.*

1. INTRODUCTION

Additive manufacturing (AM) technology allows components with complex geometry to be manufactured using a layer-by-layer construction. As feedstock, the technology enables the processing of powders or wires from different metallic materials, such as nickel alloys, titanium, aluminum, and stainless steel (Benakis et al., 2020; Karapuzha et al., 2021; Lashgari et al., 2021; Oropeza et al., 2020; Park et al., 2021; Riquelme et al., 2021; Wan et al., 2022). With the capability of processing different metallic alloys, AM can be employed in repairing and remanufacturing damaged parts. This becomes relevant for complex and high-value parts, which would be expensive and time-consuming to be replaced (Priarone et al., 2021). In refurbishing components, directed energy deposition (DED) is used to add layers of materials to rebuild worn areas of operating parts (Chen et al., 2022; Sahoo and Tripathy, 2020).

DED is an AM technology in which the deposited material is directed by a nozzle and is melted by an energy source, which can be a plasma arc, laser beam, and electron beam (TWI, 2020). As a general observation, the use of metal powder provides better accuracy and surface finish, but at a lower deposition rate than those used for depositing wire feedstock. Although for both materials (powder and wire) post-processing machining is essential for obtaining the final geometry and surface finish (Priarone et al., 2021). Notwithstanding the advantages of processing near final geometries without the need for expensive tooling, it is of relevance to control the presence of common defects in AM

including crack formation, pores, inclusions and delamination that strongly depend on the processing parameters must be considered (Li et al., 2021).

Processing parameters also affect the geometrical features of the deposited layer, namely layer height and width, penetration and as a consequence dilution, in repair operations, these contribute to control the deposit geometry. Furthermore, processing parameters influence the microstructure of the deposited material and have a significant impact on the properties of the material, such as hardness and wear resistance. To make the most of the technology, research has endeavored to optimize the processing parameters for different materials deposited with a variety of energy sources (Bharath et al., 2008; Kumar et al., 2021; Momin et al., 2022; Sadasivam and Amirthalingam, 2022; Wei et al., 2018; Yadav et al., 2019).

In comparison with the laser beam, plasma arc techniques, such as plasma transferred arc (PTA), offer higher deposition rates, good homogeneity and low oxides content, being a competitive alternative for repairing damaged parts (Cardozo et al., 2019). However, there is a lack of a systematic investigation on the PTA-DED of AISI 316L that offers information on the processing parameters selection. In particular, for repair operations, the first deposited layer has a two-fold impact on a successful refurbishing of a part: interaction with the original material and it sets a reference for subsequently deposited layers. Thus, in the present study, PTA is used to deposit single tracks of AISI 316L on AISI 304L. A design of experiments (DoE) is carried out to assess the effects of deposition current and speed on the coating hardness and geometry.

2. MATERIALS AND METHODS

Single layers of gas-atomized AISI 316L stainless steel powder (75-250 µm) were deposited by PTA on AISI 304L plates (70 x 30 x 10 mm). To evaluate the effects of deposition parameters on geometry and hardness, four levels of deposition current and three levels of deposition speed were selected, the processing parameters are shown in Tab. 1.

Figure 1 shows the geometrical features measured in the cross-section of the single-track, namely height, width, penetration, reinforcement, dilution, and wettability. The hardness and the geometrical features were measured for all experiments in the full factorial design of experiments.

Table 1. PTA deposition parameters.

Parameter	Value
Protective gas	Argon 99%
Carrier gas flow (l/min)	0.8
Plasma gas flow (l/min)	2.0
Shield gas flow (l/min)	15.0
Nozzle-plate distance (mm)	10
Powder flow rate (g/min)	10
Deposition current (A)	60, 90, 120, 150
Deposition speed (mm/min)	100, 150, 200

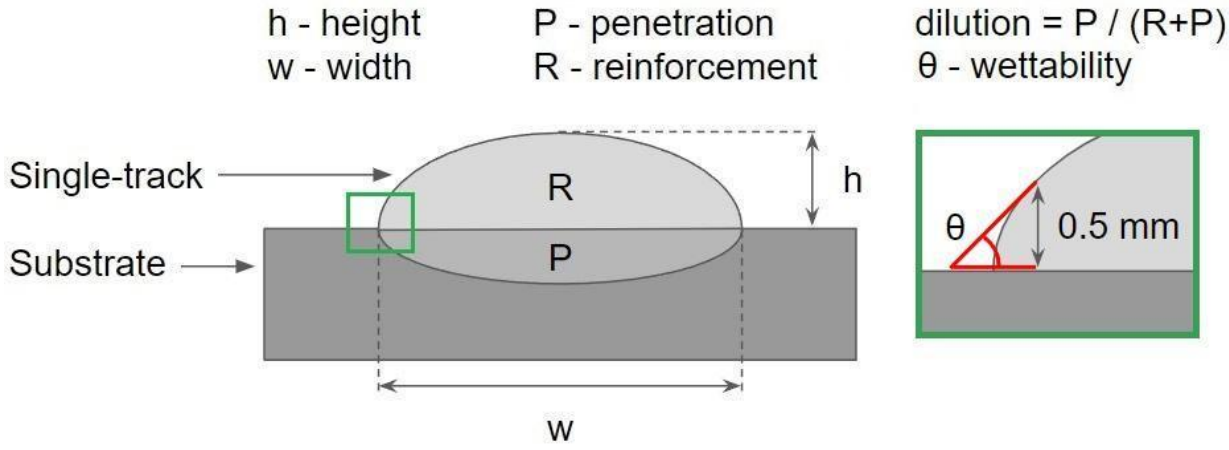

Figure 1. Single-track geometric features.

3. RESULTS AND DISCUSSIONS

The full factorial experiment was carried out at various combinations of deposition parameters by varying deposition current and speed. Table 2 presents the measured responses of the deposited single-tracks obtained at 12 combinations of parameters, which were repeated in 3 different cross-sections.

Table 2. Experimental conditions and measured responses.

Experiment	Speed (mm/min)	Current (A)	Height (mm)	Width (mm)	Wettability (º)	Reinforcement (mm²)	Penetration (mm²)	Dilution (%)	Hardness Vickers (HV 0,3)
			2,524	3,712	-	10,254	-	-	169
1	100	60	2,531	3,704	-	10,169	-	-	174
			2,512	3,735	-	10,310	-	-	178
			2,269	5,931	73,11	11,315	0,251	2,17	190
2	100	90	2,276	5,938	52,80	12,123	0,231	1,87	174
			2,281	5,856	51,00	11,822	0,181	1,51	178
			1,863	9,484	36,90	12,460	1,552	11,08	193
3	100	120	1,856	9,413	40,32	12,422	1,587	11,33	175
			1,863	9,475	42,96	12,679	1,521	10,71	178
			1,505	12,036	22,90	12,635	6,053	32,39	189
4	100	150	1,499	11,972	22,56	12,610	5,904	31,89	189
			1,508	11,999	25,75	12,804	5,998	31,90	179
			1,975	3,075	-	5,873	-	-	189
5	150	60	1,983	3,065	-	5,798	-	-	174
			1,971	3,095	-	5,901	-	-	172
			1,724	5,253	58,93	7,161	-	-	186
6	150	90	1,758	5,039	61,19	7,084	-	-	168
			1,725	5,268	53,18	7,210	-	-	177
			1,422	7,631	34,68	8,288	0,815	8,95	184
7	150	120	1,415	7,591	32,10	8,207	0,756	8,43	183
			1,436	7,583	33,51	8,359	0,776	8,49	177
			1,222	9,444	22,43	8,062	4,430	35,46	193
8	150	150	1,243	9,480	25,30	8,379	4,438	34,63	187
			1,219	9,462	22,32	8,163	4,453	35,30	183
			1,596	3,275	-	4,755	-	-	173
9	200	60	1,587	3,265	-	4,686	-	-	169
			1,599	3,283	-	4,781	-	-	177
			1,520	4,862	39,73	5,913	-	-	189
10	200	90	1,532	4,450	46,99	5,601	-	-	173
			1,532	4,450	46,99	5,601	-	-	173
			1,183	6,663	33,18	5,918	0,800	11,91	178
11	200	120	1,169	6,649	27,11	5,867	0,805	12,07	181
			1,160	6,707	25,95	5,917	0,768	11,49	183
			1,017	8,448	17,81	6,087	3,695	37,77	196
12	200	150	1,036	8,485	18,82	6,369	3,388	34,72	180
			1,025	8,476	17,83	6,227	3,316	34,75	183

The optical microscopies of the single-track cross-sections are shown in Fig. 2. It reveals a lack of fusion for the tracks deposited at a lower current (60 A) that are detached from the substrate. Lack of fusion was also identified at the following deposition with 90 A, and the faster speeds tested, 150 and 200 mm/min, as a consequence of insufficient energy per unit length. The cross-sections of the processed layers reveal that both current and speed have a great impact on the geometry of the deposited single-tracks.

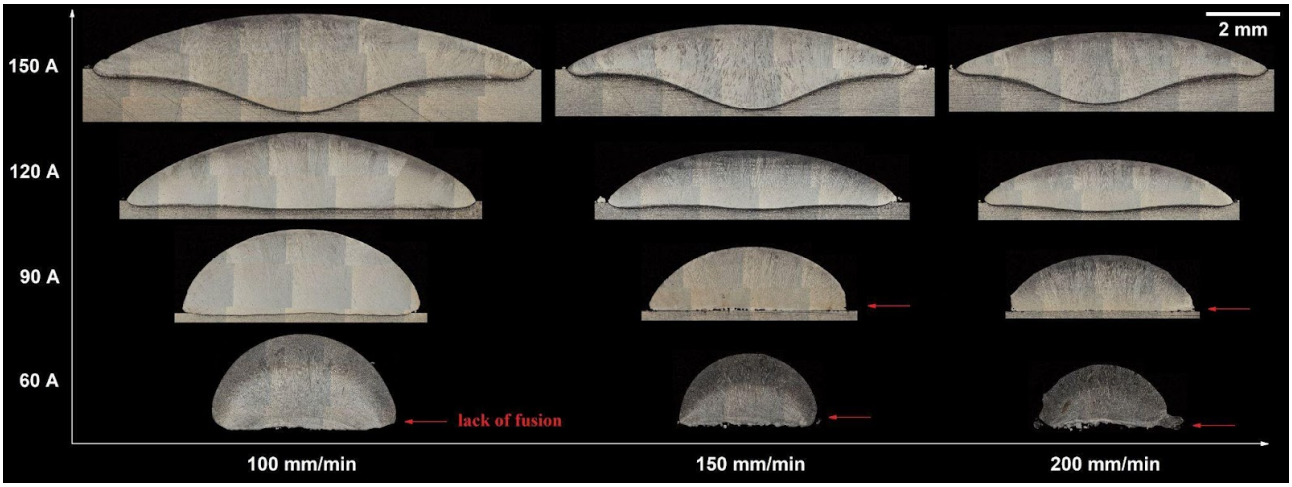

Figure 2. Optical microscopies of the single-track cross-sections.

Process maps of deposition current and speed, Figure 3 shows the contour plots of the measured geometrical features and hardness. When deposition speed is increased, less powder is fed into the melt pool per length unit, since the powder flow rate (10 g/min) is kept constant. As a result, higher deposition speeds lead to lower track heights (Fig. 3a) and lower track widths (Fig. 3b). As expected, a decrease in reinforcement area (Fig. 3d) is observed with an increase in deposition speed. Furthermore, higher deposition speed causes a reduction in energy per unit length, slightly decreasing the penetration area measured (Fig. 3e). For the tested conditions, dilution (Fig. 3f) remains almost constant with changes in speed, since both reinforcement and penetration decrease with higher deposition speed (Santos et al. 2019).

Alongside speed, deposition current also highly impacts the single-track geometry. When the deposition current is increased, more energy is available per unit length, leading to higher temperatures in the melt pool. As a consequence, higher deposition currents lead to lower wettability angles (Fig. 3c), decreasing track height (Fig. 3a), and substantially increasing the measured track width (Fig. 3b). Although keeping the powder flow rate constant, increasing deposition current slightly increases reinforcement area (Fig. 3d), this can be explained by the better capturing of the metallic powder, since higher temperatures lead to a wider melt pool (Fig. 2). Higher currents lead to an increase in both penetration and dilution (Fig. 3e and Fig. 3f) since more energy is available at the melt pool (Yaedu and d'Oliveira, 2003; Takano et al., 2008).

Analysis of variance (ANOVA) was used to quantify the impact of both individual and combined deposition parameters. Tables 3-9 show the ANOVA data for the measured responses. At Tab. 3, it is seen that both speed (46,66%) and current (50,65%) significantly contributed to the track height response. Whereas track width (Tab. 4) and wettability (Tab. 5) were mainly influenced by deposition current (86,73% and 91,92%, respectively), which highlights the effect of the energy input on these variables. The fact that the powder flow rate per length unit depends on the speed is emphasized in Tab. 6, where reinforcement is highly impacted by deposition speed (89,94%). In turn, penetration (Tab. 7) and dilution (Tab. 8) were shown to be dependent on heat input, since deposition current has the maximum contribution (92,08% and 99,22%, respectively).

Since the feedstock and the substrate have different chemical compositions, the coating hardness is directly impacted by dilution (Takano et al., 2008). As aforementioned, dilution was not impacted by deposition speed, therefore hardness measured at the single-track cross-section was not affected by deposition speed in the tested range (Fig. 3g). Increasing deposition current increases the measured hardness (Fig. 3g). This is a surprising result because a higher heat input leads to a slower cooling rate compromising the refinement of the solidification structure accounting for a lower hardness (Kumar et al., 2013). However, results showed that the increase in hardness is associated with an increase in dilution with the substrate material suggesting that alloying elements from the substrate increased solid solution saturation and the hardness of the coatings (Ramakrishnan et al., 2021).

The ANOVA data for the measured hardness is shown in Tab. 9. As expected, deposition speed has no significant effect on the measured hardness, since the P-value of 0,93 > 0,05. Also, the deposition current contribution on hardness is lower than the standard deviation contribution (33,24% and 62,37%, respectively), which means that the standard deviation of the measured hardness surpassed the variation with the selected range of deposition parameters tested.

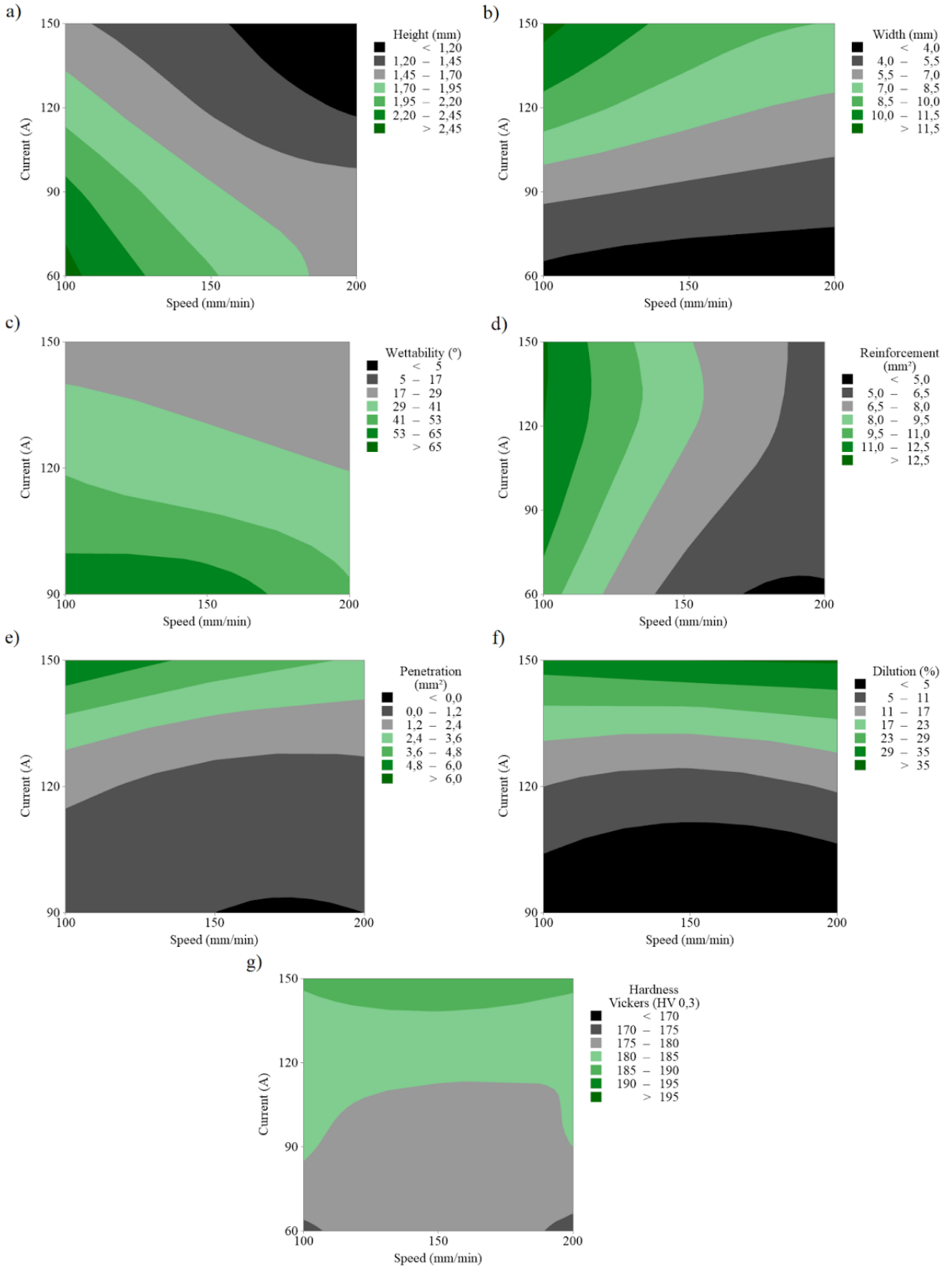

Figure 3. Contour plot of (a) Height, (b) Width, (c) Wettability, (d) Reinforcement, (e) Penetration, (f) Dilution, and (g) Hardness Vickers.

Table 3. Analysis of variance data for height.

Source	DF	Sum of Squares	Mean Square	F-Value	P-Value	Contribution %
Model	11	6,58	0,60	3419,47	<0,001	-
Speed	2	3,07	1,54	8780,89	<0,001	**46,66**
Current	3	3,34	1,11	6354,55	<0,001	**50,65**
Speed*Current	6	0,17	0,03	164,80	<0,001	2,63
Error	24	0,00	0,00			0,06
Total	35	6,59				100,00

Table 4. Analysis of variance data for width.

Source	DF	Sum of Squares	Mean Square	F-Value	P-Value	Contribution %
Model	11	263,95	24,00	4256,28	<0,001	-
Speed	2	25,50	12,75	2261,09	<0,001	9,65
Current	3	229,04	76,35	13542,03	<0,001	**86,73**
Speed*Current	6	9,42	1,57	278,47	<0,001	3,57
Error	24	0,14	0,01			0,05
Total	35	264,09				100,00

Table 5. Analysis of variance data for wettability.

Source	DF	Sum of Squares	Mean Square	F-Value	P-Value	Contribution %
Model	11	14151,30	1286,48	71,89	<0,001	-
Speed	2	448,90	224,47	12,54	<0,001	3,08
Current	3	13402,80	4467,60	249,65	<0,001	**91,92**
Speed*Current	6	299,60	49,93	2,79	0,033	2,05
Error	24	429,50	17,90			2,95
Total	35	14580,80				100,00

Table 6. Analysis of variance data for reinforcement.

Source	DF	Sum of Squares	Mean Square	F-Value	P-Value	Contribution %
Model	11	267,97	24,36	1007,46	<0,001	-
Speed	2	241,52	120,76	4994,19	<0,001	**89,94**
Current	3	24,66	8,22	340,00	<0,001	9,18
Speed*Current	6	1,78	0,30	12,27	<0,001	0,66
Error	24	0,58	0,02			0,22
Total	35	268,55				100,00

Table 7. Analysis of variance data for penetration.

Source	DF	Sum of Squares	Mean Square	F-Value	P-Value	Contribution %
Model	11	139,46	12,68	3041,51	<0,001	-
Speed	2	4,91	2,45	588,69	<0,001	3,52
Current	3	128,51	42,83	10276,40	<0,001	**92,08**
Speed*Current	6	6,04	1,01	241,67	<0,001	4,33
Error	24	0,10	0,00			0,07
Total	35	139,56				100,00

Table 8. Analysis of variance data for dilution.

Source	DF	Sum of Squares	Mean Square	F-Value	P-Value	Contribution %
Model	11	6995,12	635,92	2049,48	<0,001	-
Speed	2	5,72	2,86	9,21	<0,001	0,08
Current	3	6948,18	2316,06	7464,34	<0,001	**99,22**
Speed*Current	6	41,22	6,87	22,14	<0,001	0,59
Error	24	7,45	0,31			0,11
Total	35	7002,57				100,00

Table 9. Analysis of variance data for hardness.

Source	DF	Sum of Squares	Mean Square	F-Value	P-Value	Contribution %
Model	11	705,64	64,15	1,32	0,275	-
Speed	2	7,06	3,53	0,07	0,93	0,38
Current	3	623,19	207,73	4,26	0,015	33,24
Speed*Current	6	75,39	12,57	0,26	0,951	4,02
Error	24	1169,33	48,72			**62,37**
Total	35	1874,97				100,00

4. CONCLUSIONS

A systematic investigation on the PTA-DED of AISI 316L was carried out in this study. The key findings for the tested conditions are as follows:

- AISI 316L powder was successfully deposited by PTA, resulting in sound single-track coatings. The exception was the coatings processed with 60 A, which resulted in insufficient dilution, detaching the coating from the substrate.
- The contour plots can be used to predict the hardness and the geometric response of AISI 316L coating to process parameters within the tested range.
- Single track height is governed by both deposition current and speed, which decreases by increasing any of the two tested factors.
- Deposition current was found to be the most influential parameter affecting width, as a result of a decrease in wettability angle. In addition, penetration, and consequently dilution, is mostly influenced by deposition current.
- On the other hand, deposition speed was discovered to be the most significant factor influencing reinforcement area, since the powder flow rate was kept constant.
- For the tested conditions, the variation in deposition speed did not change the hardness of the AISI 316L coating. However, the dispersion of the measured hardness is very significant for the test conditions used.

ACKNOWLEDGEMENTS

The authors acknowledge CAPES, CNPq and the Laboratory of Additive Manufacturing and Surface Engineering (LAMSE) of UFPR.

5. REFERENCES

Benakis, M., Costanzo, D., Patran, A., 2020. Current mode effects on weld bead geometry and heat affected zone in pulsed wire arc additive manufacturing of Ti-6-4 and Inconel 718. *Journal of Manufacturing Processes*, Vol. 60, n. 18, p. 61-74.

Bharath, R. R., Ramanathan, R., Sundararajan, B., & Srinivasan, P. B., 2008. Optimization of process parameters for deposition of Stellite on X45CrSi93 steel by plasma transferred arc technique. *Materials & Design*, Vol. 29, Issue 9, p. 1725–1731.

Cardoso, E., Rios, S., Pardal, G., Ganguly, S., D'Oliveira, A.S.C.M., 2019. Additive Techniques to Refurbish Ni Based Components. *Soldagem e Inspeção*, Vol. 24, p. 8.

Chen, X., Wang, C., Ding, J., Bridgeman, P., & Williams, S., 2022. A three-dimensional wire-feeding model for heat and metal transfer, fluid flow, and bead shape in wire plasma arc additive manufacturing. *Journal of Manufacturing Processes*, Vol. 83, p. 300–312.

Karapuzha, A.S., Fraser, D., Zhu, Y., Wu, X., Huang, A., 2021. Effect of solution heat treatment and hot isostatic pressing on the microstructure and mechanical properties of Hastelloy X manufactured by electron beam powder bed fusion. *Journal of Materials Science and Technology*, Vol. 98, n. 6, p. 99-117.

Kumar, R., & K Arya, H., 2013. Experimental Determination of Cooling Rate and its Effect on Microhardness in Submerged Arc Welding of Mild Steel Plate (Grade c-25 as per IS 1570). *Journal of Material Science & Engineering*, Vol. 03, Issue 02.

Kumar, P., Sawant, M. S., & Jain, N. K., 2021. Optimization of process parameters in micro-plasma transferred arc deposition process for cobalt-based alloy. *Materials Today: Proceedings*, Vol. 44, pp. 1681–1686.

Lashgari, H.R., Li, S., Kong, C., Asnavandi, M., Zangeneh, S.H., 2021. Rotary friction welding of additively manufactured 17-4PH stainless steel. *Journal of Manufacturing Processes*, Vol. 64, n. 16, p. 1517-1528.

Li, R., Jin, M., Paquit, V.C., 2021. Geometrical defect detection for additive manufacturing with machine learning models. *Materials & Design*, Vol. 206, n. 20.

Momin, A.G., Khatri, B.C., Chaudhari, M., Shah, U., Valaki, J., 2022. Parameters for cladding using plasma transfer arc welding – A critical. *Materials Today: Proceedings*.

Oropeza, D., Hofmann, D.C., Williams, K., Firdosy, S., Bordeenithikasem, P., Sokoluk, M., Liese, M., Liu, J., Li, X., 2020. Welding and additive manufacturing with nanoparticle-enhanced aluminum 7075 wire. *Journal of Alloys and Compounds*, Vol. 834, n. 13.

Park, S.H., Son, S.J., Lee, S.B., Yu, J.H., Ahn, S.J., Choi, Y.S., 2021. Surface machining effect on material behavior of additive manufactured SUS 316L. *Journal of Materials Research and Technology*, Vol. 13, n. 22, p. 38-47.

Priarone, P. C., Campatelli, G., Catalano, A. R., Baffa, F., 2021. Life-cycle energy and carbon saving potential of Wire Arc Additive Manufacturing for the repair of mold inserts. *CIRP Journal of Manufacturing Science and Technology*, Vol. 35, p. 943–958.

Ramakrishnan et al., 2021. Experimental investigation on mechanical properties of TIG welded dissimilar AISI 304 and AISI 316 stainless steel using 308 filler rod. Materials Today: Proceedings, Vol. 45, p. 8207–8211.

Riquelme, A., Candela, C.S.R., Ram, J., 2021. Influence of process parameters in additive manufacturing of highly reinforced 316L / SiCp composites. *Journal of Manufacturing Processes*, Vol. 299, n. 14.

Sadasivam, P., Amirthalingam, M., 2022. Design and fabrication of micro-plasma transferred wire arc additive manufacturing system. *CIRP Journal of Manufacturing Science and Technology*, Vol. 37, p. 185–195.

Sahoo, A., Tripathy, S., 2021. Development in plasma arc welding process: A review. *Materials Today: Proceedings*, Vol. 41, p. 363–368.

Santos, A.X., Maciel, T.M., Costa, J.D., Sousa, M.B., Prasad, S., Campos, A.R.N., Santana, R.A.C., 2019. Study on influence of the PTA-P welding process parameters on corrosion behavior of Inconel 625 coatings. *Matéria (Rio de Janeiro)*, Vol. 24.

Takano, E.H., Queiroz, D., d'Oliveira, A.S.C.M., 2008. Avaliação dos Parâmetros de Processamento por PTA nas Superfícies Processadas. *Soldagem & Inspeção*, Vol. 13, p. 210-218.

TWI, 2020. What is directed energy deposition (DED)? The Welding Institute. 27 Nov. 2022 <https://www.twi-global.com/technical-knowledge/faqs/directed-energy-deposition>.

Wan, H.Y., Yang, W.K., Wang, L.Y., Zhou, Z.J., Li, C.P., Chen, G.F., Lei, L.M., Zhang, G.P., 2022. Toward qualification of additively manufactured metal parts: Tensile and fatigue properties of selective laser melted Inconel 718 evaluated using miniature specimens. *Journal of Materials Science & Technology*, Vol. 97, n. 29, p. 239-253.

Wei, Y., Wei, X., Chen, B., Zuo, J., Ma, T., & Shen, J., 2018. Parameter optimization for tungsten carbide/Ni-based composite coating deposited by plasma transferred arc hardfacing. *Transactions of Nonferrous Metals Society of China*, Vol. 28, Issue 12, p. 2511–2519.

Yadav, S., Jinoop, A. N., Sinha, N., Paul, C. P., & Bindra, K. S., 2020. Parametric investigation and characterization of laser directed energy deposited copper-nickel graded layers. *The International Journal of Advanced Manufacturing Technology*, Vol. 108, Issues 11–12, p. 3779–3791.

Yaedu, A.E. and d'Oliveira, A.S.C.M., 2003. *Influência do substrato na deposição de Stellite 1 com plasma de arco transferido*. Master degree dissertation, Federal University of Paraná, Curitiba.

6. RESPONSIBILITY NOTICE

The authors are the only ones responsible for the printed material included in this paper.